ZEUS-prel-06-020

Submitted to the
XXXIII International Conference on High Energy Physics
ICHEP06 (July 26-August 2, Moscow, Russia)

Abstract: **Session: Hard QCD**

Jet cross sections in charged current $e^{-}p$ deep inelastic scattering at HERA II

ZEUS Collaboration

Abstract

Differential inclusive-jet cross sections have been measured in charged current deep inelastic $e^{-}p$ scattering in the kinematic range given by $Q^2 > 200$ GeV^2 and $y < 0.9$, where Q^2 is the exchanged boson virtuality and y is the inelasticity, with the ZEUS detector at HERA using an integrated luminosity of 125 pb^{-1}. Jets were identified using the k_T cluster algorithm in the longitudinally inclusive mode in the laboratory frame. Cross sections are presented as functions of Q^2, Bjorken x, the jet transverse energy, $E_T^{\rm jet}$ and pseudorapidity, $\eta^{\rm jet}$. Jets were selected with $E_T^{\rm jet} > 11$ GeV and $-1 < \eta^{\rm jet} < 2.5$. The unpolarised-corrected measurements are compared to leading-logarithm parton-shower Monte Carlo calculations and to measurements in $e^{+}p$ collisions. Results for negatively and positively polarised electron beams are also presented.

1 Introduction

Jet production in charged-current (CC) deep inelastic ep scattering (DIS) provides a testing ground for QCD and for the electroweak sector of the Standard Model (SM). Up to leading order (LO) in the strong coupling constant, α_s, jet production in CC DIS proceeds via the quark-parton model ($Wq \to q$), the QCD-Compton ($Wq \to qg$) and W-gluon fusion ($Wg \to q\bar{q}$) processes. Thus, differential cross sections for jet production are sensitive to α_s and the mass of the propagator, M_W, which are fundamental parameters of the theory.

The large centre-of-mass energy available at the HERA ep collider ($\sqrt{s} \approx 300$ GeV) extended the kinematic region for studying CC DIS with respect to fixed-target neutrino scattering experiments [1] by about two orders of magnitude in the virtuality of the exchanged boson, Q^2, and to lower values of the fraction of the proton's momentum carried by the struck parton, x. Measurements of the CC DIS cross section at HERA [2–4] at high Q^2 demonstrated the presence of a space-like propagator with a finite mass, consistent with that of the W boson. Since 2002, HERA is running with longitudinally-polarised electron or positron beams. Measurements of the total cross section for positive and negative values of the longitudinal polarisation of the beams have been found to be in good agreement with the predictions of the SM [5, 6].

At HERA, multijet structures have been observed in CC DIS [3, 7, 8] at large Q^2 and jet shapes and subjet multiplicities have been measured [8, 9] and compared with NC DIS processes [9,10]. The subjet multiplicities have been used to extract a value of $\alpha_s(M_Z)$ [8].

In this paper, measurements are presented of inclusive-jet cross sections in CC e^-p DIS in the laboratory frame. Jets are identified with the k_T cluster algorithm [11] in the longitudinally invariant inclusive mode [12]. The jets were selected with jet transverse energy $E_T^{\rm jet} > 11$ GeV and pseudorapidity[1] $-1 < \eta^{\rm jet} < 2.5$. The measurements are given for $Q^2 > 200$ GeV^2 and $y < 0.9$, where y is the inelasticity, and presented as functions of Q^2, Bjorken x, $E_T^{\rm jet}$ and $\eta^{\rm jet}$. The measurements are compared to leading-logarithm parton-shower Monte Carlo (MC) models. The measurements, restricted to $E_T^{\rm jet} > 14$ GeV and $-1 < \eta^{\rm jet} < 2$, are compared to similar previous measurements in CC e^+p DIS [8]. Results for negative and positive longitudinally-polarised electron beams are also presented.

[1] The ZEUS coordinate system is defined as right-handed with the Z-axis pointing in the proton beam direction, hereafter referred to as forward, and the X-axis horizontal, pointing towards the centre of HERA.

2 Data selection and jet search

The data were collected during the running period 2004-2005, when HERA operated with protons of energy $E_p = 920$ GeV and electrons of energy $E_e = 27.5$ GeV, and correspond to an integrated luminosity of 125.4 ± 4.4 pb^{-1}. Samples of negatively (positively) polarised electron beams with an integrated luminosity of 79.3±2.8 (46.1±1.6) pb^{-1} and luminosity-weighted average polarisation of $P_e^{\rm neg} = -0.27 \pm 0.01$ ($P_e^{\rm pos} = +0.33 \pm 0.02$) were analysed. The electron beam polarisation was measured using the HERA Compton polarimeters [13].

A detailed description of the ZEUS detector can be found elsewhere [14, 15]. A three-level trigger was used to select events online [15]. Two different trigger selections were used, one which relied only on large $p_{T,\rm miss}$ and E_T, where $p_{T,\rm miss}$ is the missing transverse momentum as measured with the ZEUS calorimeter (CAL) ($p_{T,\rm miss} \equiv \sqrt{p_X^2 + p_Y^2}$) and E_T is the total transverse energy as measured in the CAL. The alternative trigger selection required additionally the presence of at least one high transverse-energy jet. Events from CC DIS interactions were selected offline using criteria similar to those of an earlier publication [8]. The kinematic variables Q^2 and y were reconstructed using the method of Jacquet-Blondel [16], which uses the information from the hadronic energy flow of the event, and corrected for detector effects as described elsewhere [9].

The main selection criteria are:

- $p_{T,\rm miss} > 11$ GeV;
- $p_{T,\rm miss}/E_T > 0.5$;
- the vertex position along the beam axis in the range $-35 < Z < 33$ cm;
- at least one track associated with the vertex;
- the number of tracks not associated with the vertex must be less than 20% of the total number of tracks;
- the difference $\Delta\varphi$ between the azimuth of the net transverse momentum as measured by the tracks associated with the vertex and the azimuth measured by the CAL has been required to fulfill $|\Delta\varphi| < 1$ rad;
- $P_{T,\rm tracks}/p_{T,\rm miss} > 0.1$, where $P_{T,\rm tracks}$ is the net transverse momentum of the tracks associated with the vertex (this condition was not applied if $p_{T,\rm miss} > 25$ GeV);
- events were removed from the sample if there was an isolated electron candidate with energy above 10 GeV;
- $Q^2 > 200$ GeV^2;
- $y < 0.9$.

Jets were searched for in the pseudorapidity (η) - azimuth (ϕ) plane of the laboratory frame using the longitudinally invariant k_T-cluster algorithm. This algorithm combines particles with a small relative distance d_{ij},

$$d_{ij} = \min(E_{T,i}, E_{T,j})^2 \cdot ((\eta_i - \eta_j)^2 + (\phi_i - \phi_j)^2),$$

where $E_{T,i}$, η_i and ϕ_i are the transverse energy, pseudorapidity and azimuth of particle i. The axis of the jet was defined according to the Snowmass convention [17], where $\eta^{\rm jet}$ ($\phi^{\rm jet}$) is the transverse-energy weighted mean pseudorapidity (azimuth) of all the particles belonging to that jet. The jets have been reconstructed using the CAL and corrected for detector effects to yield jets of hadrons. Events with at least one jet of $E_T^{\rm jet} > 11$ GeV and $-1 < \eta^{\rm jet} < 2.5$ were retained. The final sample consisted of $N_{\rm data}^{\rm neg} = 3249$ and $N_{\rm data}^{\rm pos} = 1016$ events, where $N_{\rm data}^{\rm neg(pos)}$ are the number of data events selected from runs with negatively (positively) polarised electron beams.

3 Monte Carlo simulation

Samples of events were generated to determine the response of the detector to jets of hadrons and to evaluate the correction factors necessary to obtain the hadron-level inclusive-jet cross sections. The CC DIS events were generated using the LEPTO 6.5 program [18] interfaced to HERACLES 4.6.1 [19] via DJANGOH 1.3 [20]. The HERACLES program includes first-order electroweak radiative corrections, vertex and propagator terms, and two-boson exchange. The CTEQ5D [21] proton parton distribution functions (PDFs) were used. The QCD radiation was modelled with the colour-dipole model (CDM) [22] by using the ARIADNE 4.08 program [23] including the boson-gluon-fusion process. As an alternative, samples of events were generated using the LEPTO model which is based on first-order QCD matrix elements and parton showers (MEPS). For the generation of the LEPTO samples, the option for soft-colour interactions was switched off. In both cases, fragmentation into hadrons was performed using the Lund string model [24] as implemented in JETSET 7.4 [25].

The jet search was performed on the MC events using the energy measured in the CAL cells in the same way as for the data. The same jet algorithm was also applied to the final-state hadrons to obtain the predictions at the hadron level. For both the CDM and MEPS event samples, a good description of the measured distributions for the kinematic and jet variables was obtained.

To correct the data to the hadron level, multiplicative correction factors, defined as the ratio of the measured quantities for jets of hadrons over the same quantity for jets at detector level, were estimated by using the CDM samples as default. The samples of

MEPS were used as an estimation of the uncertainty on the modelling of the parton shower.

4 Systematic uncertainties

The following sources of systematic uncertainty were considered for the measurements of the cross sections:

- the uncertainty in the absolute energy scale of the jets was estimated to be $\pm 3\%$;
- the differences in the results obtained by using either CDM or MEPS to correct the data for detector effects were taken as systematic uncertainties;
- the uncertainty in the reconstruction of the kinematic variables due to that in the absolute energy scale of the CAL was estimated by varying the energy variables measured with the CAL by $\pm 3\%$ in the MC samples;
- the selection cut of $p_{T,\mathrm{miss}} > 11$ GeV was changed to 10 GeV and 12 GeV in data and MC events;
- the photoproduction background was estimated to have a $\pm 5\%$ effect on the cross sections;
- the uncertainty in the simulation of the trigger was estimated by using two different trigger selections in data and MC events (see Section 2).

The systematic uncertainties not associated with the absolute energy scale of the jets were added in quadrature to the statistical uncertainties and are shown in the figures as error bars. The uncertainty due to the absolute energy scale of the jets is shown separately as a shaded band in each figure, due to the large bin-to-bin correlation. In addition, there was an overall normalisation uncertainty of 3.5% from the luminosity determination. The relative uncertainty in the measured polarisation was 5%.

5 Results

Using the selected data sample, differential inclusive-jet cross sections were measured in the kinematic regime given by $Q^2 > 200$ GeV^2 and $y < 0.9$. The cross sections were determined for those jets with $E_T^{\mathrm{jet}} > 11$ GeV and $-1 < \eta^{\mathrm{jet}} < 2.5$. Figure 1 shows the unpolarised-corrected CC $e^- p$ DIS inclusive-jet differential cross sections as functions of η^{jet}, E_T^{jet}, Q^2 and Bjorken x. The unpolarised-corrected cross section for observable A ($A = \eta^{\mathrm{jet}}$, E_T^{jet}, Q^2 and Bjorken x) was obtained via

$$\frac{d\sigma}{dA} = \frac{N_{\rm data}^{\rm unpol}}{\mathcal{L} \cdot \Delta A} \cdot \frac{N_{\rm MC}^{\rm had}}{N_{\rm MC}^{\rm det}},$$

where

$$N_{\rm data}^{\rm unpol} = \frac{N_{\rm data}^{\rm neg}}{1 - P_e^{\rm neg}} + \frac{N_{\rm data}^{\rm pos}}{1 - P_e^{\rm pos}},$$

$\mathcal{L}$ is the total integrated luminosity and ΔA is the bin width.

The measured $d\sigma/d\eta^{\rm jet}$ has a maximum at $\eta^{\rm jet} \sim 0.75$. The measured $d\sigma/dE_T^{\rm jet}$ exhibits a fall-off of two orders of magnitude for $E_T^{\rm jet} \gtrsim 20$ GeV. For $11 < E_T^{\rm jet} \lesssim 20$ GeV, this distribution displays almost no dependence on $E_T^{\rm jet}$. The cross section as a function of Q^2 shows a less rapidly fall-off than what is observed in NC DIS processes due to the presence of the massive W propagator. The measured cross section in Fig. 1d shows that the Bjorken x values accessible by the data are within the range $0.003 < x < 0.3$.

The predictions of the leading-logarithm parton-shower MC models of CDM and MEPS are compared to the data in the figure. The lower part of the figure shows the relative difference between the data and the CDM predictions. The CDM and MEPS predictions are very similar in this kinematic regime and give a reasonable description of the $\eta^{\rm jet}$ and Bjorken x measured cross sections. However, the measured cross sections have a different shape than the predictions as functions of $E_T^{\rm jet}$ and Q^2: they are above (below) the predictions for low (high) $E_T^{\rm jet}$ and Q^2.

Figure 2 shows the CC negatively and positively polarised e^-p DIS inclusive-jet differential cross sections as functions of $\eta^{\rm jet}$, $E_T^{\rm jet}$, Q^2 and Bjorken x. The predictions of the leading-logarithm parton-shower MC model of CDM are compared to the data in the figure. The lower part of the figure shows the ratio of the cross section for negatively and positively polarised electron beams, which is agreement with the measured polarisation ratio, $(1 - P_e^{\rm neg})/(1 - P_e^{\rm pos}) = 1.90 \pm 0.07$. The uncertainty in the polarisation measurement is included as a hatched band in Fig. 2. The total jet cross sections in the kinematic regime given by $Q^2 > 200$ GeV^2, $y < 0.9$, $E_T^{\rm jet} > 11$ GeV and $-1 < \eta^{\rm jet} < 2.5$ are

$$\sigma_{\rm jets}(P_e = -0.27 \pm 0.01) = 71.3 \ \pm 1.2 \text{ (stat.) } \pm 3.6 \text{ (syst.) } \pm 0.3 \text{ (E scale) pb},$$

$$\sigma_{\rm jets}(P_e = +0.33 \pm 0.02) = 38.7 \ \pm 1.2 \text{ (stat.) } \pm 2.0 \text{ (syst.) } \pm 0.2 \text{ (E scale) pb},$$

in agreement with the MC predictions: $\sigma_{\rm jets}(P_e = -0.27) = 75$ pb and $\sigma_{\rm jets}(P_e = +0.33) = 40$ pb. The systematic uncertainty quoted above includes also the uncertainty due to the luminosity measurement.

Jet cross sections in e^-p are expected to be approximately twice the magnitude of those in e^+p, since the two reactions probe different proton parton content. A previous ZEUS analysis [8] measured inclusive-jet cross sections using a sample of e^+p data with 111 pb^{-1} of integrated luminosity in the same kinematic range as presented here for jets with $E_T^{\rm jet} > 14$ GeV and $-1 < \eta^{\rm jet} < 2$. Using the selected data sample restricted to these $E_T^{\rm jet}$ and $\eta^{\rm jet}$ ranges, unpolarised-corrected differential inclusive-jet cross sections were measured. Figure 3 shows the measured e^-p cross sections compared to those for e^+p [8] as functions of $\eta^{\rm jet}$, $E_T^{\rm jet}$ and Q^2. The lower part of the figure shows the ratio between the cross sections in e^-p and e^+p collisions. The ratio as a function of $\eta^{\rm jet}$ is constant and ≈ 2, as predicted by the MC models. The ratio as a function of $E_T^{\rm jet}$ (Q^2) increases as $E_T^{\rm jet}$ (Q^2) increases, in agreement with the prediction. The increase at high values of $E_T^{\rm jet}$ and Q^2 is expected due to the increasing contribution from the valence-quark densities in the proton at high x and the fact that both reactions are sensitive to different quark flavours. The behaviour observed in the ratio of the measured cross sections as a function of Q^2 is similar to the ratio of u and d parton densities.

6 Summary

Measurements of polarised and unpolarised-corrected differential inclusive-jet cross sections in CC e^-p DIS production have been made using 125.4 pb^{-1} of data collected with the ZEUS detector at HERA for the first time. These cross sections are directly sensitive to the flavour content of the proton. The cross sections refer to jets identified in the laboratory frame with the k_T cluster algorithm in the longitudinally invariant inclusive mode and selected with $E_T^{\rm jet} > 11$ GeV and $-1 < \eta^{\rm jet} < 2.5$. The measurements were made in the kinematic region defined by $Q^2 > 200$ GeV^2 and $y < 0.9$.

Differential inclusive-jet cross sections were measured as functions of $\eta^{\rm jet}$, $E_T^{\rm jet}$, Q^2 and Bjorken x. The cross sections as functions of $\eta^{\rm jet}$ and Bjorken x are reasonably well described by leading-logarithm parton-shower Monte Carlo models, whereas the measured cross sections as functions of $E_T^{\rm jet}$ and Q^2 have a different shape than the predictions.

The ratio of the cross section for negatively and positively polarised electron beams is well described by the predictions. The total jet cross sections in the kinematic regime given by $Q^2 > 200$ GeV^2, $y < 0.9$, $E_T^{\rm jet} > 11$ GeV and $-1 < \eta^{\rm jet} < 2.5$ are

$$\sigma_{\rm jets}(P_e = -0.27 \pm 0.01) = 71.3 \ \pm 1.2 \text{ (stat.) } \pm 3.6 \text{ (syst.) } \pm 0.3 \text{ (E scale) pb},$$

$$\sigma_{\rm jets}(P_e = +0.33 \pm 0.02) = 38.7 \ \pm 1.2 \text{ (stat.) } \pm 2.0 \text{ (syst.) } \pm 0.2 \text{ (E scale) pb}.$$

The unpolarised-corrected inclusive-jet cross sections in e^-p have been compared to measurements in e^+p collisions in the kinematic regime given by $Q^2 > 200$ GeV^2, $y < 0.9$, $E_T^{\rm jet} > 14$ GeV and $-1 < \eta^{\rm jet} < 2$. The ratio as a function of $\eta^{\rm jet}$ is contant and ≈ 2, as predicted by the MC models. The ratio as a function of $E_T^{\rm jet}$ (Q^2) increases as $E_T^{\rm jet}$ (Q^2) increases, in agreement with the expected increased contribution from the valence-quark densities in the proton at high x and the fact that both reactions are sensitive to different quark flavours.

References

[1] CDHS Coll., H. Abramowicz et al., Z. Phys. **C 25**, 29 (1984);
CDHSW Coll., J.P. Berge et al., Z. Phys. **C 49**, 187 (1991);
CCFR Coll., E. Oltman et al., Z. Phys. **C 53**, 51 (1992);
BEBC Coll., G.T. Jones et al., Z. Phys. **C 62**, 575 (1994).

[2] H1 Coll., T. Ahmed et al., Phys. Lett. **B 324**, 241 (1994);
H1 Coll., S. Aid et al., Z. Phys. **C 67**, 565 (1995);
H1 Coll., S. Aid et al., Phys. Lett. **B 379**, 319 (1996);
ZEUS Coll., M. Derrick et al., Phys. Rev. Lett. **75**, 1006 (1995).

[3] ZEUS Coll., M. Derrick et al., Z. Phys. **C 72**, 47 (1996).

[4] ZEUS Coll., J. Breitweg et al., Eur. Phys. J. **C 12**, 411 (2000).

[5] H1 Coll., A. Aktas et al., Phys. Lett. **B 634**, 173 (2006).

[6] ZEUS Coll., S. Chekanov et al., Phys. Lett. **B 637**, 210 (2006).

[7] H1 Coll., C. Adloff et al., Eur. Phys. J. **C 19**, 249 (2001).

[8] ZEUS Coll., J. Chekanov et al., Eur. Phys. J. **C 31**, 149 (2003).

[9] ZEUS Coll., J. Breitweg et al., Eur. Phys. J. **C 8**, 367 (1999).

[10] ZEUS Coll., S. Chekanov et al., Phys. Lett. **B 558**, 41 (2003).

[11] S. Catani et al., Nucl. Phys. **B 406**, 187 (1993).

[12] S.D. Ellis and D.E. Soper, Phys. Rev. **D 48**, 3160 (1993).

[13] M. Beckmann et al., Nucl. Inst. Meth. **A 479**, 334 (2002);
D.P. Barber et al., Nucl. Inst. Meth. **A 329**, 79 (1993).

[14] ZEUS Coll., M. Derrick et al., Phys. Lett. **B 293**, 465 (1992).

[15] ZEUS Coll., U. Holm (ed.), *The ZEUS Detector*. Status Report (unpublished), DESY (1993), available on `http://www-zeus.desy.de/bluebook/bluebook.html`.

[16] F. Jacquet and A. Blondel, *Proc. of the Study for an ep Facility for Europe*, U. Amaldi (ed.), p. 391. Hamburg, Germany (1979). Also in preprint DESY 79/48.

[17] J.E. Huth et al., *Research Directions for the Decade. Proc. of Summer Study on High Energy Physics, 1990*, E.L. Berger (ed.), p. 134. World Scientific (1992). Also in preprint FERMILAB-CONF-90-249-E.

[18] G. Ingelman, A. Edin and J. Rathsman, Comp. Phys. Comm. **101**, 108 (1997).

[19] A. Kwiatkowski, H. Spiesberger and H.-J. Möhring, Comp. Phys. Comm. **69**, 155 (1992);

H. Spiesberger, *An Event Generator for ep Interactions at HERA Including Radiative Processes (Version 4.6)*, 1996, available on
`http://www.desy.de/~hspiesb/heracles.html`.

[20] K. Charchuła, G.A. Schuler and H. Spiesberger, Comp. Phys. Comm. **81**, 381 (1994);
H. Spiesberger, HERACLES *and* DJANGOH*: Event Generation for ep Interactions at HERA Including Radiative Processes*, 1998, available on
`http://www.desy.de/~hspiesb/djangoh.html`.

[21] H.L. Lai et al., Eur. Phys. J. **C 12**, 375 (2000).

[22] Y. Azimov et al., Phys. Lett. **B 165**, 147 (1985);
G. Gustafson, Phys. Lett. **B 175**, 453 (1986);
G. Gustafson and U. Pettersson, Nucl. Phys. **B 306**, 746 (1988);
B. Andersson et al., Z. Phys. **C 43**, 625 (1989).

[23] L. Lönnblad, Comp. Phys. Comm. **71**, 15 (1992);
L. Lönnblad, Z. Phys. **C 65**, 285 (1995).

[24] B. Andersson et al., Phys. Rep. **97**, 31 (1983).

[25] T. Sjöstrand, Comp. Phys. Comm. **39**, 347 (1986);
T. Sjöstrand and M. Bengtsson, Comp. Phys. Comm. **43**, 367 (1987).

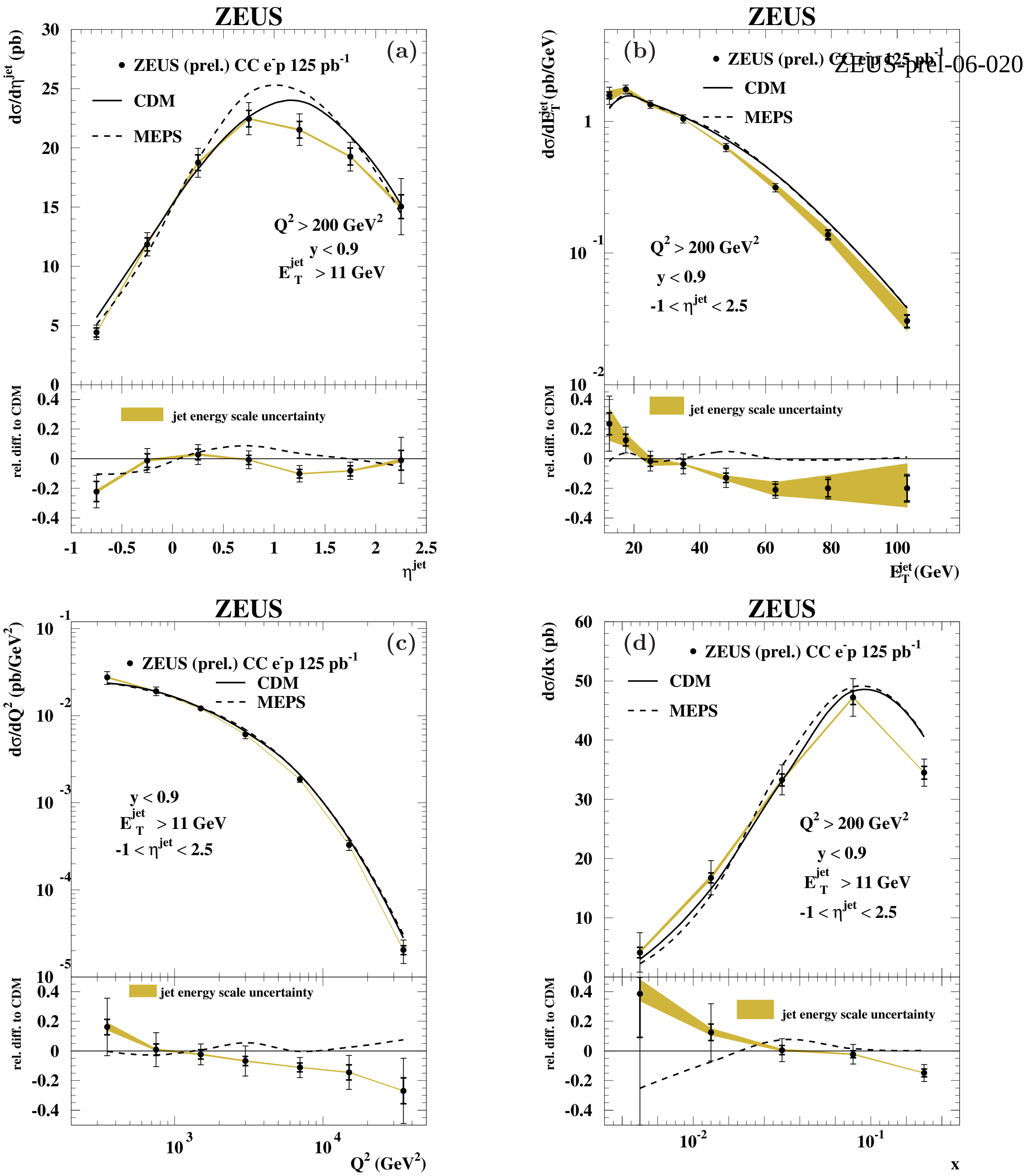

Figure 1: *Measured unpolarised-corrected inclusive-jet cross sections in CC e^-p DIS for jets with $E_T^{\rm jet} > 11$ GeV and $-1 < \eta^{\rm jet} < 2.5$ in the kinematic regime given by $Q^2 > 200$ GeV^2 and $y < 0.9$ as functions of (a) $\eta^{\rm jet}$, (b) $E_T^{\rm jet}$, (c) Q^2 and (d) Bjorken x (dots). The inner error bars represent the statistical uncertainties of the data, and the outer error bars show the statistical and systematic uncertainties —not associated with the absolute energy scale of the jets— added in quadrature. The shaded band displays the uncertainty due to the absolute energy scale of the jets. For comparison, the predictions of the leading-logarithm parton-shower Monte Carlo models of CDM (solid lines) and MEPS (dashed lines) are included. The lower part of the figures displays the relative difference between the measured cross section and the corresponding predictions of CDM (dots); the relative difference between the predictions of MEPS and CDM is also shown (dashed lines).*

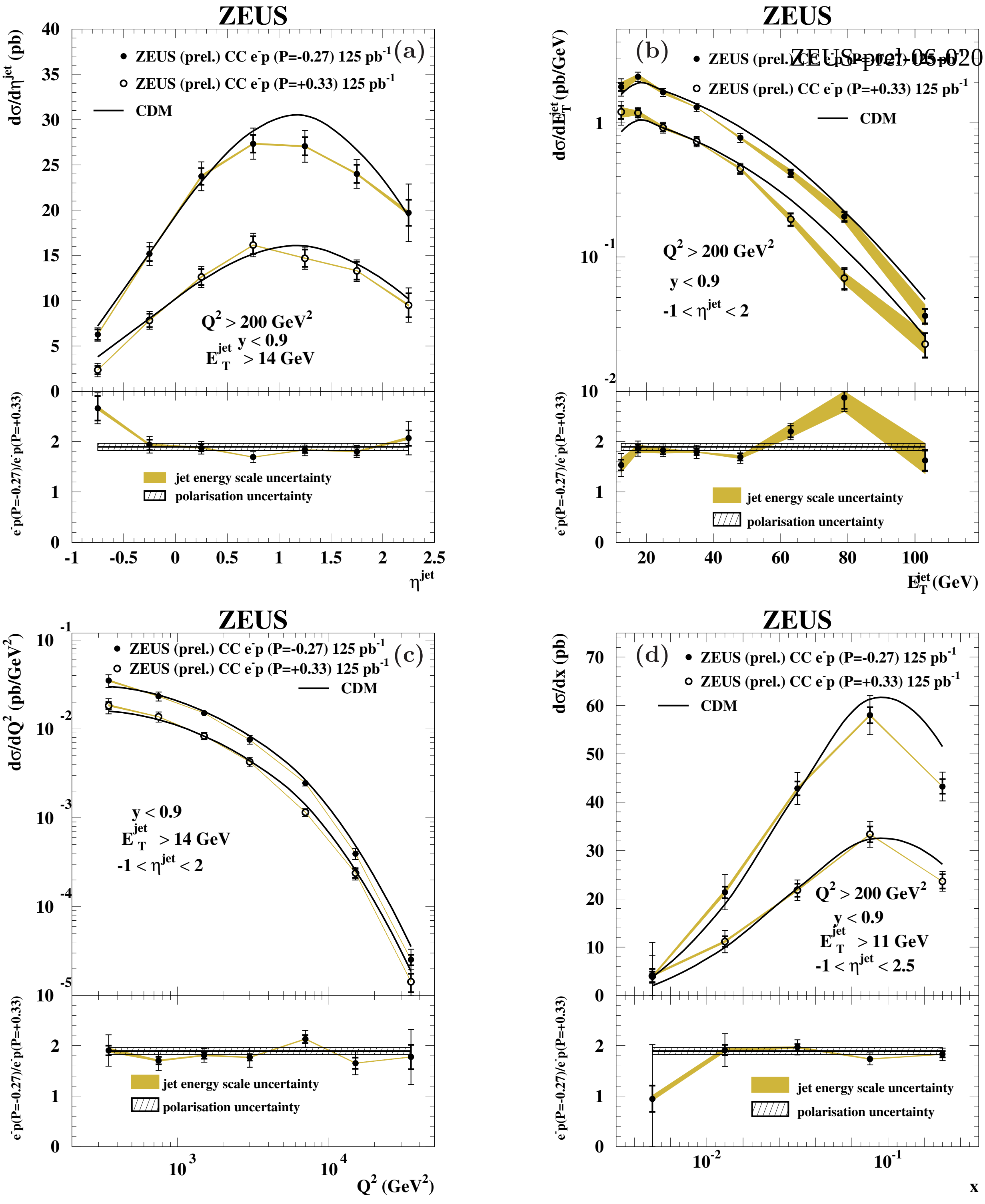

Figure 2: *Measured inclusive-jet cross sections in CC e^-p DIS for jets with $E_T^{\rm jet} > 11$ GeV and $-1 < \eta^{\rm jet} < 2.5$ in the kinematic regime given by $Q^2 > 200$ GeV^2 and $y < 0.9$ as functions of (a) $\eta^{\rm jet}$, (b) $E_T^{\rm jet}$, (c) Q^2 and (d) Bjorken x for negative (dots) and positive (white circles) polarised electron beams. For comparison, the predictions of the leading-logarithm parton-shower Monte Carlo model of CDM (solid lines) are included. The lower part of the figures displays the ratio of the cross sections for negatively and positively electron beams. The hatched band represents the uncertainty in the polarisation measurement. Other details as in the caption to Fig. 1.*

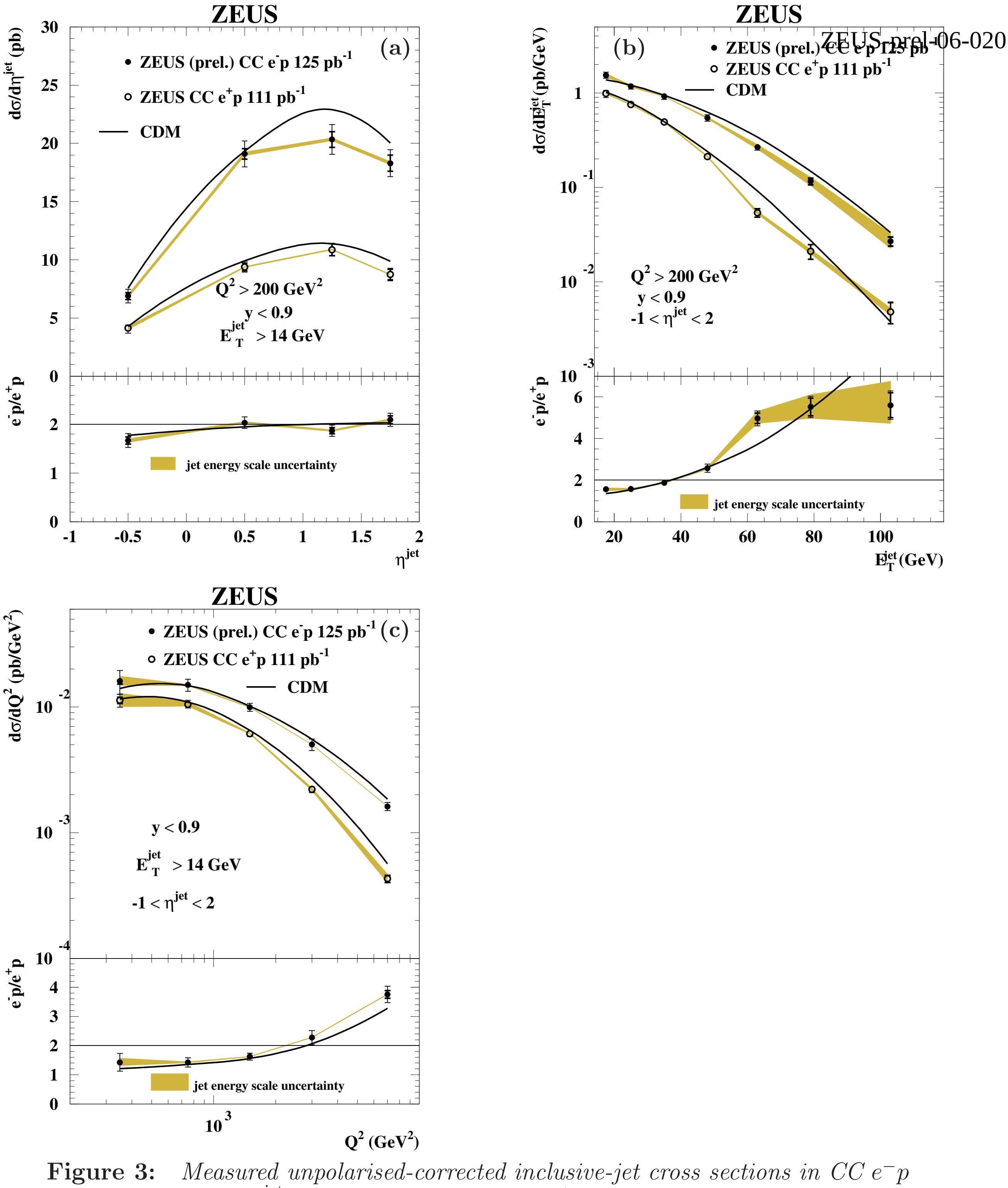

Figure 3: *Measured unpolarised-corrected inclusive-jet cross sections in CC e^-p DIS for jets with $E_T^{\rm jet} > 14$ GeV and $-1 < \eta^{\rm jet} < 2$ in the kinematic regime given by $Q^2 > 200$ GeV^2 and $y < 0.9$ as functions of (a) $\eta^{\rm jet}$, (b) $E_T^{\rm jet}$ and (c) Q^2 (dots). The measured cross sections for e^+p data (white circles) are also shown. For comparison, the predictions of the leading-logarithm parton-shower Monte Carlo model of CDM (solid lines) are included. The lower part of the figures displays the ratio of the cross sections for e^-p and e^+p collisions. Other details as in the caption to Fig. 1.*